

The Robotic Vision Scene Understanding Challenge

David Hall, Ben Talbot, Suman Raj Bista, Haoyang Zhang, Rohan Smith,
Feras Dayoub, Niko Sünderhauf

September 14, 2020

Abstract

Being able to explore an environment and understand the location and type of all objects therein is important for indoor robotic platforms that must interact closely with humans. However, it is difficult to evaluate progress in this area due to a lack of standardized testing which is limited due to the need for active robot agency and perfect object ground-truth. To help provide a standard for testing scene understanding systems, we present a new robot vision scene understanding challenge using simulation to enable repeatable experiments with active robot agency. We provide two challenging task types, three difficulty levels, five simulated environments and a new evaluation measure for evaluating 3D cuboid object maps. Our aim is to drive state-of-the-art research in scene understanding through enabling evaluation and comparison of active robotic vision systems.

1 Introduction

One of the long-held goals in robotics is to have autonomous systems which can reliably work alongside humans within unstructured environments such as homes and offices. A basic building block of such a system is scene understanding, or, knowing what objects exist in its environment and where they are. In research, this problem of scene understanding is typically viewed through the lens of semantic sim-

This research was conducted by the Australian Research Council Centre of Excellence for Robotic Vision (project number CE140100016), and supported by the QUT Centre for Robotics. Email: d20.hall@qut.edu.au

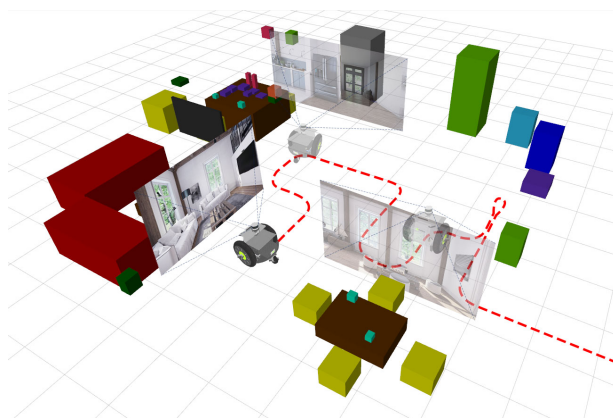


Figure 1: Visual representation of the new scene understanding challenge. A robotic agent must actively explore an environment to produce a 3D cuboid map of all objects of interest. Image by shgraphicdesign.net

taneous localisation and mapping (SLAM) and is tested using standard datasets like KITTI [1], Sun RGBD [2], and Scene Net [3]. Whilst these are beneficial for algorithm comparison, they are static datasets showing a fixed sequence of sensor data and miss a critical component of robotic systems, namely active agency.

To address this issue, we present a new benchmark challenge for active robotic vision research in scene understanding to enable easy comparison of active systems. The challenge is summarized visually in Figure 1. Key aspects and contributions of our new challenge are as follows:

- Definition of two scene understanding tasks:

Semantic SLAM and Scene Change Detection (SCD).

- Use of simulation to enable repeatable evaluation of active robotic systems
- Use of tiered difficulty levels to enable ablation studies and easy participation by non-roboticists
- Use of discretised action space controlled through a simple API
- Use of a new evaluation measure for evaluating object maps from Semantic SLAM

2 Related Work

Our scene understanding challenges intersects two areas of research. Namely, the creation of standardized challenges and benchmarks for robotics, and the evaluation of sparse semantic SLAM systems.

2.1 Robotics challenges

Quantitative evaluation and comparison is uncommon in the field of robotics research when compared to computer vision, due largely to difficulties in standardization of hardware, software, and/or environments [4]. Due to this, robotics challenges typically focus on adding constraints and standards to scenarios that enable comparison.

A common constraint placed on robotics challenges is to use only pre-recorded data. This enables analysis of an algorithm's ability to interpret data for a given task. This is the approach used by KITTI [1], Sun RGBD [2], Cityscape [5], SceneNet [3], and Oxford RobotCar [6] datasets which enable multiple tasks to be evaluated such as object tracking, visual odometry, SLAM, semantic segmentation, etc. However, the constraint of using pre-recorded data is limiting, as a critical component of robotics is that the system is an active agent in its environment, capable of making decisions based upon their observations.

To enable active agents and perform holistic testing of a robot system at a task, some challenges choose

to only constrain the testing environment. Challenges such as RoboCup@Home [7], the DARPA challenge [8], and the Amazon picking challenge [9] have a fixed environment where competitors can bring their robot systems on a given challenge day for comparison and ranking of a specific problem. This method provides the most flexibility but challenges are infrequent, have high costs for hardware, engineering resources and potentially travel, and allow mostly for system-level analysis and comparison rather than any specific area of robotics research.

To analyse specific areas of research in a standardized way with active agency included, some approaches provide access to fixed robot platforms available in a fixed set of environments. This can be done by remote access to a platform as done by RoboThor [10], iGibson [11], and the real robot challenge¹ and is a very promising area of robotics testing research. However, currently it is more common to use simulation tools to simulate both robots and environments. This is used not only by systems designed only to work in simulation like AI-Habitat [12], AI2Thor [13], embodied question answering [14], and the active vision dataset [15], but also by systems that enable sim-to-real transfer like AirSim [16], CARLA [17], Isaac [18], and the aforementioned, iGibson [11] and RoboThor [10]. Simulation enables rapid prototyping and comparison of robotic algorithms which consider the active nature of robotics without high implementation costs and, when using the correct tools, without sacrificing the ability to transfer techniques to robot platforms in the real world. Simulation therefore is the tool we use for our challenge.

2.2 Semantic SLAM Evaluation

Common metrics of evaluating visual SLAM methods are absolute trajectory error (ATE) and the relative pose error (RPE) [19]. These are focused on trajectory estimation, comparing global positional offsets, and local motion errors respectively, between estimated and ground-truth trajectories. These are typically expressed as a root-mean-square-error (RMSE)

¹<https://real-robot-challenge.com/en>

measure [19, 20]. These are used frequently as at least part of a SLAM evaluation process. While beneficial in testing localisation, these are not required for our purposes as we are focused on the quality of object mapping rather than robot trajectory.

Densely reconstructed SLAM maps are commonly evaluated in a pixel-wise fashion. When performing a purely spatial analysis, mean distances [21] and absolute relative depth distance [22] have been used to evaluate maps. If semantics are considered, the two major approaches are to either reproject the classified 3D points into 2D and use 2D semantic segmentation evaluation measures, or to adapt 2D measures for a 3D space. The reprojection approach is seen in [23, 24] and the adaptation of 2D measures for 3D is shown in [25, 26, 27]. These either supplant purely spatial analyses or add to them with extra semantic analysis. While useful in their given fields, we are focused on sparse object maps that lend themselves easily to rapidly optimized large-scale SLAM systems [28, 29, 30].

Sparse object-oriented semantic SLAM systems are a relatively recent addition in the field of SLAM research, but contain similar splits in evaluation process as well as utilising some methods found in object detection research. If object semantics are not evaluated as part of the map, accuracy of centroid estimation and 3D intersection over union (IoU) are frequently used to evaluate the spatial quality of the map [31, 32, 33]. In addition, if the representations are not axis aligned, measures such as average orientation similarity [34, 31], and average angular offsets of the main axis [33] are additional measures when using bounding box and quadric object representations respectively. Borrowing from object detection literature, the fusion of semantic and spatial analysis is typically done using adaptations of mean average precision (mAP) with 3D IoU used in place of 2D IoU [35, 36, 37, 38]. This is effective in combining these two important aspects of sparse object-oriented mapping, however, mAP has some drawbacks that might be detrimental within this setting. It cannot be broken down to show performance at the disparate aspects of the map (spatial and semantic quality), depends on a tunable threshold to define success, and can obscure false positive object proposals [39]. This

final point can be doubly critical for evaluating object maps, which, when compared to object detection datasets numbering in the many thousands of images and objects, are smaller in scale which has been suggested could increase the magnitude of said problems [39]. Due to these known weaknesses in mAP, particularly with respect to how they would interplay with the scene understanding challenges we propose, we are led to design our own evaluation measure outlined in Section 5.

3 Challenges

In order to address the limited tools available for reliable evaluation of active robotic systems for sparse semantic scene understanding, we present new scene understanding challenges. We define new semantic SLAM and scene change detection (SCD) scene understanding tasks to help drive robotics research. We also define three different “difficulty levels” to enable participation by non-roboticists, whilst also enabling ablation studies for scene understanding systems.

3.1 Semantic SLAM

The semantic SLAM challenge requires a robotic agent to explore a given environment and create an object map of all objects of interest (a pre-defined set of classes). In this challenge, an object map (M), as proposed by the autonomous system, is made up of a set of m objects (O) such that $M = \{O_1, O_2, O_3, \dots, O_m\}$. Every proposed object is defined by an axis-aligned cuboid ($C = \{c_x, c_y, c_z, e_x, e_y, e_z\}$), where c_x, c_y, c_z and e_x, e_y, e_z centroid and extent of the object in the global coordinate system, and a class label probability distribution (I) across all n object classes of interest, such that $O = \{C, I\}$. A visual example of a semantic SLAM object map can be seen in Figure 2a. Note that for our purposes, the representation of the ground-truth object map (\hat{M}) is likewise made up of a set of n ground-truth objects (\hat{O}). The only difference between ground-truth objects and the proposed objects output by an autonomous system is that the ground-truth class label (\hat{l}) is known such that $\hat{O} = \{C, \hat{l}\}$.

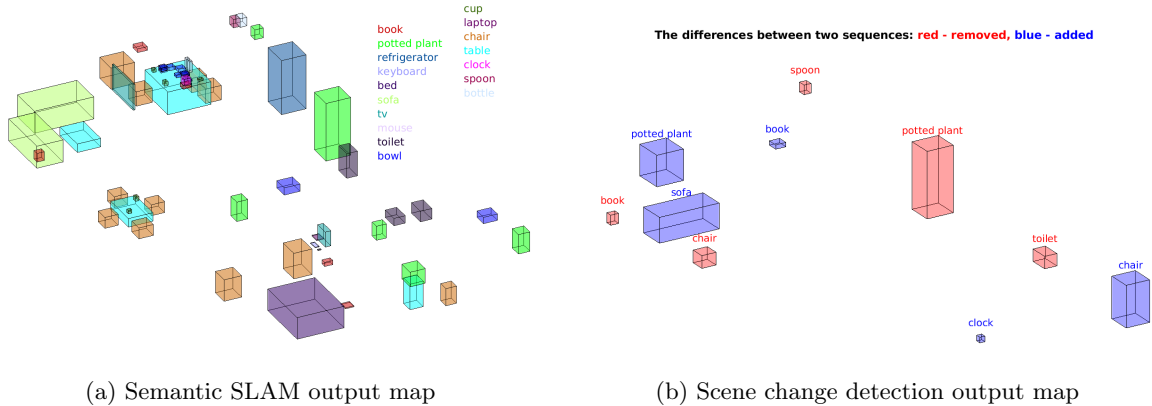


Figure 2: Examples of output from the two scene understanding tasks. In semantic SLAM (a) all object axis-aligned cuboids are mapped (colours represent classes). In scene change detection (b) only changed objects are mapped (changes shown by colour) but classes are still required.

3.2 Scene Change Detection (SCD)

In scene change detection (SCD), a robot must explore an environment at two different times, mapping any object changes between them. In this challenge, object changes consist of objects being added and removed from the environment. We leave objects moving within the environment as a consideration for future challenges. Like the semantic SLAM task, the goal in SCD is to create an object map. However, unlike semantic SLAM the object map should only contain changed objects. The definition of an object now also includes a state probability (s) giving the probability that an object was added, removed, or remained the same. This changes the object definitions for SCD to $O = \{C, l, s\}$ and $\hat{O} = \{C, \hat{l}, \hat{s}\}$ for proposed and ground-truth objects respectively, where \hat{s} is the true state of an object. A visual example of an object map for SCD is shown in Figure 2b.

3.3 Difficulty Levels

One of the novel aspects of our scene understanding challenge is the use of varying difficulty levels that not only lower the bar of entry for non-roboticist researchers, but enable some level of ablation study of the robotic system. The difficulty levels are ap-

plied across both the semantic SLAM and SCD tasks. We provide 3 levels of difficulty in this challenge, with increases in difficulty corresponding with an increased number of sub-tasks which must be considered, and increased similarity to a robotic system. This approach allows competitors to perform ablation studies for some sub-tasks, enabling determination of what systems might need to be improved upon. A summary of the difficulty levels and corresponding robotic sub-tasks to be considered is provided in Table 1.

The simplest level of difficulty is a passive mode with ground-truth pose (**Passive, GT**). At this level, the robotic agent moves between a set of pre-defined nodes. This removes the need for active agency, navigation, exploration, and obstacle avoidance. This is the most akin to other challenges and benchmarks which use pre-recorded data, beneficial as a starting point for those who have no experience controlling active agents. As ground-truth pose is provided at this level, localization also does not need to be considered. Although a useful entry point, enabling testing of object detection and mapping, this level is not very representative of robotic systems.

The medium difficulty level is an active mode with ground-truth pose (**Active, GT**). This level still provides ground-truth pose data to remove the need for

Table 1: Robot system sub-tasks that must be considered for the three different challenge difficulty levels.

	Object Detection + Mapping	Navigation + Exploration	Obstacle Avoidance	Localization
Passive, GT	✓			
Active, GT	✓	✓	✓	
Active, DR	✓	✓	✓	✓

localization, but now gives active control of the robot. This introduces the elements of needing to actively explore to find all objects of interest, as well as to avoid hitting any obstacles while traversing. While increasing difficulty, active agency is a critical part of robotic systems that must be considered for any system, making this level more representative than the previous one. However, agents operating at this difficulty are still working under ideal circumstances, always knowing precisely where they are without the need to self-localize.

The highest difficulty level is the one which most closely resembles a real robot system where the agents have active control but use dead reckoning localization (**Active, DR**). Without ground-truth pose information, the agent must self-localize using noisy pose data coming from wheel encoders. Systems that perform well at this difficulty level are considered the systems with the best chance of having similar performance under real-world conditions.

4 The Simulator System

To provide standardised environments for running repeatable experiments with active robot agents, we utilise a high-fidelity simulation system. The base simulator tool used in our system is the NVIDIA Isaac Simulator², version 2019.2 which provides robot simulation within environments rendered using Unreal Engine³. From this, we define the environments and robotic agents used to complete our scene under-

²<https://www.nvidia.com/en-us/deep-learning-ai/industries/robotics/>

³<https://www.unrealengine.com>

standing challenges.

4.1 Environments

Simulated environments consist of five base environments, each having five variations thereof, for a total of 25 environments. The five base environments are given easily identifiable names: house, miniroom, apartment, company, and office. The house and miniroom environments are provided for algorithm development, where ground-truth object maps are provided, and apartment, company and office environments are used for final testing. This provides a total of 10 environments for development and 15 for testing. It should be noted though that the size of the environments varies, with miniroom being a single small room, whereas house and company are very large environments. The environments provided are summarized in Figure 3.

The base environments are adapted from ones purchased from Evermotion⁴ and adapted to make them suitable for simple exploration by a robotic platform. The correlation of evermotion environments and their names as given in the challenge are outlined in Table 2. Adaptions made to each base environment to enable exploration include: flattening environments to enable access to elevated areas without stairs, removing doors that block important rooms, and adding walls to section off intraversable areas with built-in objects of interest that would otherwise need to be mapped.

Objects of interest are objects that are within a subset of classes from the COCO dataset. A breakdown of the classes and their frequency across all en-

⁴<https://evermotion.org/>

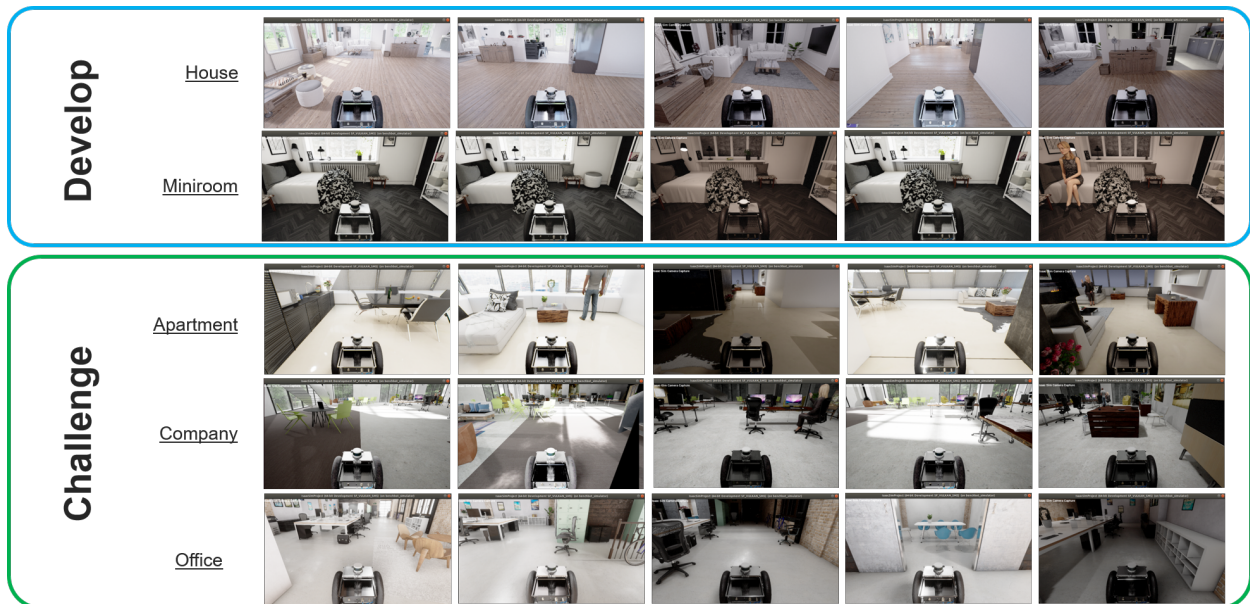


Figure 3: Environments used for scene understanding challenges. There are five variations to each base environment (named). The third and fifth variations show the environments at night.

Table 2: Evermotion environments and their corresponding names within the challenge

Evermotion	Challenge
Archinteriors Vol 2 Scene 2	House
Archinteriors Vol 3 Scene 3	Miniroom
Archinteriors Vol 1 Scene 1	Apartment
Archinteriors Vol 1 Scene 5	Company
Archinteriors Vol 1 Scene 3	Office

environment sets (base environment plus variations) is provided in Table 3. Objects are either part of these original base environments, or were purchased separately through the Unreal Marketplace.

As previously mentioned, each base environment has a set of five variations. Each variation has some different combination of objects with between 8 and 27 total object changes (added and removed) between any given pair of environment variations. As well as this, the third and fifth variation of each environment has been crafted to be an interpretation of the environment at night rather than the day as is the default. This can be seen in Figure 3. This is to add an extra element of challenge, particularly in SCD where most objects must be re-identified and mapped despite the lighting changes.

We choose environment subsets for the challenge test data for each difficulty level that maximises variation within the subset, and minimises overlap between subsets. The subsets are summarised in Table 4. Development environments do not have subsets as the intention is for people to experiment as much as they

Table 3: Distribution of all object instances across all environments: Miniroom (M), House (H), Apartment (A), Company (C) and Office (O), and total number of instances across all environments (T). Values for each environment are the total numbers across all 5 variations of each base environment.

Class	M	H	A	C	O	T
Bottle	7	15	14	1	0	37
Cup	3	25	17	21	2	68
Bowl	4	42	7	12	0	65
Spoon	3	0	0	0	0	3
Banana	1	0	4	0	0	5
Apple	4	0	10	10	0	24
Orange	3	1	1	5	3	13
Cake	0	0	0	3	0	3
Plant	9	32	29	47	19	136
Mouse	0	5	0	36	40	81
Keyboard	0	5	0	36	40	81
Laptop	1	6	3	5	2	17
Book	13	25	16	18	112	184
Clock	3	4	5	10	0	22
Chair	10	47	27	183	86	353
Table	15	21	25	57	20	138
Couch	0	11	20	5	0	36
Bed	5	5	0	0	0	10
Toilet	0	14	0	0	0	14
TV	0	10	3	39	39	91
Microwave	0	0	2	0	0	2
Toaster	2	2	4	0	0	8
Fridge	0	3	2	4	3	12
Sink	4	5	10	0	0	19
Person	2	2	6	11	0	21

wish with environment combinations when developing solutions and to enable ablation studies using the same environment at different difficulty levels.

4.2 Robot Agents

Our challenge is made possible through the use of robotic agents that can actively explore an environment to produce a semantic map. To ensure consistency in the challenge and enable the different challenge difficulties outlined previously, we define fixed sets of discretised robot controls as well as a fixed sensor suite. The sensorimotor interaction between the agent controls and sensors described below, and the underlying robot platform, are provided by the BenchBot system [40].

4.2.1 Agent Control

The challenge provides robot agents with two different types of control mechanisms: passive navigation, and active control. Passive navigation involves guiding a robot through a repeatable, pre-determined trajectory. Active control presents full control of the robot, fulfilling requests to travel explicit linear distances and angular rotations.

Under passive control, the robot travels to the next pose along a trajectory with a guaranteed maximum error of 1 cm in position and 1° in orientation. The robot begins inter-pose traversal on a move to next command, employing a pose controller to reconcile differences in current pose and desired pose. Each environment has a different trajectory with length varying from 33 to 484 poses. The distribution of trajectory lengths can be seen in Figure 4.

Active control allows the robot to respond to navigation requests like “move forward 1 m” and “rotate 60° ”. The same controller is employed as in passive control, but a dynamic goal pose is generated given the robot’s current position and requested navigation action.

Navigation commands are executed based on the robot’s odometry readings which is an important distinction for dead-reckoning modes. For example, in trying to “move forward 1 m” the robot will travel

Table 4: Distribution of simulated test environments across task and difficulty level

Task:Difficulty	Office					Apartment					Company				
	1	2	3	4	5	1	2	3	4	5	1	2	3	4	5
Sem. SLAM: Passive, GT	✓		✓			✓		✓			✓		✓		
Sem. SLAM: Active, GT		✓		✓			✓		✓			✓		✓	
Sem. SLAM: Active, DR				✓	✓				✓	✓				✓	✓
SCD: Passive, GT	✓	✓	✓			✓	✓	✓			✓	✓	✓		
SCD: Active, GT		✓	✓		✓		✓	✓		✓		✓	✓		✓
SCD: Active, DR	✓			✓	✓	✓			✓	✓	✓			✓	✓

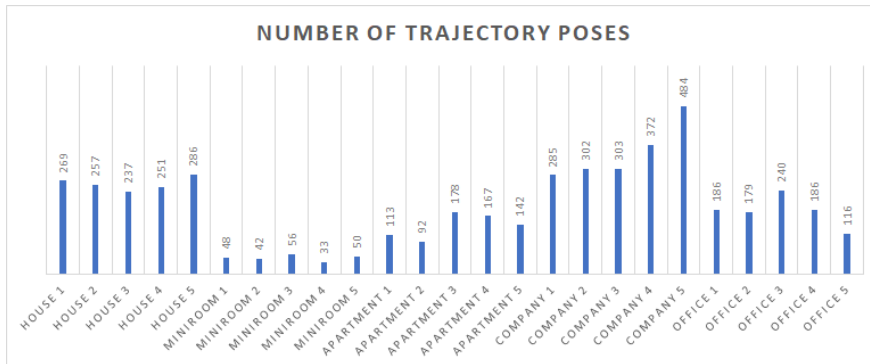


Figure 4: Number of trajectory poses for environments under passive control.

1m (± 1 cm) with respect to its odometry readings, but this could be 1.1 m in reality.

4.2.2 Agent Sensors

After each navigation action, the agent is provided with a set of observations from the robot platform’s sensor suite. Sensorimotor observations include:

- the ground-truth initial pose of the robot in the environment
- synced 960x540RGB and depth images from a simulated front-facing sensor
- calibration parameters for the RGB and depth sensors, including intrinsic and projection matrices
- a 360° flat-laser scan from a simulated Velodyne P16 lidar sensor, with a resolution of 0.4° and a maximum range of 57.29 m

- a list of 6-DOF poses for the platform including the camera, lidar, robot base, and starting pose in the global map frame.

5 Object Map Quality (OMQ) Evaluation

As our scene understanding challenges focus on the generation of cuboid object maps, we provide a new object map quality (OMQ) evaluation measure to evaluate map accuracy. The measure is heavily based on the probability-based detection quality (PDQ) evaluation measure designed for probabilistic object detection [39], now adapted for evaluating 3D object maps for Semantic SLAM. Adapting OMQ for SCD will be outlined in Section 5.1.

The process for OMQ is as follows. For each object in the proposed map, we calculate a pairwise object quality (pOQ) between them and each ground-truth

object in the ground-truth map. The pOQ score is simply the geometric mean of a spatial and label quality (Q_{Sp} and Q_L respectively). This is formally expressed for the i -th proposed object (O_i) and j -th ground-truth object (\hat{O}_j) as

$$pOQ(O_i, \hat{O}_j) = \sqrt{Q_{Sp}(O_i, \hat{O}_j) \cdot Q_L(O_i, \hat{O}_j)}. \quad (1)$$

Unlike in PDQ, for OMQ spatial quality is simply the 3D IoU score between ground-truth and proposed object cuboids as is used in other works [31, 33]. Label quality is calculated in the same manner as PDQ, taking the probability given to the correct class.

$$Q_L(O_i, \hat{O}_j) = \mathbf{l}_i(\hat{l}_j) \quad (2)$$

Once all pairwise scores are calculated, objects in the proposed map are optimally assigned to objects in the ground-truth map. From this we attain a list of “true positive” quality scores with non-zero quality assignments (\mathbf{q}^{TP}), and the number of “true positives” (N_{TP}), false negatives (N_{FN}), and false positives N_{FP} . Unlike in the original PDQ paper [39], we also create a list of false positive costs (\mathbf{c}_{FP}) for all false positives in order to weigh overconfident false positives as worse than low-confidence false positives. This is in alignment with later versions of PDQ found in the latest versions of their code⁵ but not formally expressed in any paper. False positive cost is simply the maximum label probability given to a non-background (BG) class label, expressed formally as

$$FP_{cost}(O_i) = \max_{l \neq BG} \mathbf{l}_i(l). \quad (3)$$

This is what is currently used for PDQ in the probabilistic object detection (PrOD) challenges⁶.

The final OMQ score is calculated as an average of “true positive” pOQ scores, across all “true positives” false negatives and false positives, with false positives weighted according to their aforementioned cost. This is formally expressed as

$$OMQ(M, \hat{M}) = \frac{\sum_{i=1}^{N_{TP}} \mathbf{q}(i)}{N_{TP} + N_{FN} + \sum_{j=1}^{N_{FP}} \mathbf{c}_{FP}(j)}. \quad (4)$$

⁵<https://github.com/jskinn/rvchallenge-evaluation>

⁶<https://competitions.codalab.org/competitions/2059>

It should be noted that as with PDQ, the spatial and label qualities can be used as separate quality measures for fine-grained analysis.

5.1 Adapting OMQ for SCD

While the previous definition of OMQ is suited for Semantic SLAM analysis, the OMQ measure is easily adapted for SCD by adding a state quality term to accommodate the confidence given that an object has been added or removed. State quality (Q_{St}) operates the same way as label quality, simply being the confidence given to the correct state of the object in question (added or removed). This is formally expressed as

$$Q_{St}(O_i, \hat{O}_j) = \mathbf{s}_i(\hat{s}_j). \quad (5)$$

The pOQ score for SCD then becomes the geometric mean between the label, spatial, and state qualities as follows

$$pOQ_{SCD} = \sqrt[3]{Q_{Sp} \cdot Q_L \cdot Q_{St}}. \quad (6)$$

Note that above, all components are equations dependant on i -th proposed object and j -th ground-truth object as in equation (1) but is abbreviated here for spacing reasons. Also note that including state quality will change the relative importance of the spatial and semantic aspects of quality from that seen in Semantic SLAM due to averaging over three terms instead of two.

State probability also effects the false positive cost of OMQ. False positive cost becomes the geometric mean of the maximum non-background label probability, and the maximum state probability that is not “same” (added or removed). Formally this is

$$FP_{SCDcost}(O_i) = \sqrt{\max_{l \neq BG} \mathbf{l}_i(l) \cdot \max_{s \neq \text{same}} \mathbf{s}_i(s)}. \quad (7)$$

With this consideration, the worst false positives are certain about what the object is and that said object was added or removed. As we use the geometric mean, if either of these is very low, the cost of the false positive will be greatly reduced.

Beyond these changes to false pOMQ and false positive cost, OMQ is calculated as normal for SCD as for Semantic SLAM.

6 Summary and Future Work

We show a new robotic vision scene understanding challenge utilising high-fidelity simulation to enable active robot agency. Unlike static datasets which show a pre-recorded set of data, in our challenge the robot agents have autonomy and must actively explore environments to map out objects and detect changes in scenes. We outline two new challenge tasks, three difficulty levels that enable ablation studies and contributions from non-roboticists, our simulated environments and robotic agents, and our new object map quality evaluation measure. Future works should build on the basic ideas covered in this paper, expanding both the realism and variety of environments and robotic platforms used as the current data pool is limited when compared to the variety of static datasets. Further expansions could utilise ideas such as object interactivity and dynamic obstacles as used in other works. Finally, providing sim-to-real transfer of solutions, as is made possible by tools like BenchBot, should be pursued further to reliably test solutions in real-world settings.

References

- [1] A. Geiger, P. Lenz, C. Stiller, and R. Urtasun, "Vision meets robotics: The kitti dataset," *International Journal of Robotics Research (IJRR)*, 2013.
- [2] S. Song, S. P. Lichtenberg, and J. Xiao, "Sun rgb-d: A rgb-d scene understanding benchmark suite," in *Proceedings of the IEEE conference on computer vision and pattern recognition*, 2015, pp. 567–576.
- [3] J. McCormac, A. Handa, S. Leutenegger, and A. J. Davison, "Scenenet rgb-d: Can 5m synthetic images beat generic imagenet pre-training on indoor segmentation?" 2017.
- [4] A. P. del Pobil, R. Madhavan, and E. Messina, "Benchmarks in robotics research," in *Workshop IROS*. Citeseer, 2006.
- [5] M. Cordts, M. Omran, S. Ramos, T. Rehfeld, M. Enzweiler, R. Benenson, U. Franke, S. Roth, and B. Schiele, "The cityscapes dataset for semantic urban scene understanding," in *Proc. of the IEEE Conference on Computer Vision and Pattern Recognition (CVPR)*, 2016.
- [6] W. Maddern, G. Pascoe, C. Linegar, and P. Newman, "1 Year, 1000km: The Oxford RobotCar Dataset," *The International Journal of Robotics Research (IJRR)*, vol. 36, no. 1, pp. 3–15, 2017. [Online]. Available: <http://dx.doi.org/10.1177/0278364916679498>
- [7] "Robocup@home 2019: Rules and regulations (draft)," http://www.robocupathome.org/rules/2019_rulebook.pdf, 2019.
- [8] E. Krotkov, D. Hackett, L. Jackel, M. Perschbacher, J. Pippine, J. Strauss, G. Pratt, and C. Orłowski, "The darpa robotics challenge finals: Results and perspectives," *Journal of Field Robotics*, vol. 34, no. 2, pp. 229–240, 2017.
- [9] N. Correll, K. E. Bekris, D. Berenson, O. Brock, A. Causo, K. Hauser, K. Okada, A. Rodriguez, J. M. Romano, and P. R. Wurman, "Analysis and observations from the first amazon picking challenge," *IEEE Transactions on Automation Science and Engineering*, vol. 15, no. 1, pp. 172–188, 2016.
- [10] M. Deitke, W. Han, A. Herrasti, A. Kembhavi, E. Kolve, R. Mottaghi, J. Salvador, D. Schwenk, E. VanderBilt, M. Wallingford *et al.*, "Robothor: An open simulation-to-real embodied ai platform," in *Proceedings of the IEEE/CVF Conference on Computer Vision and Pattern Recognition*, 2020, pp. 3164–3174.
- [11] F. Xia, W. B. Shen, C. Li, P. Kasimbeg, M. E. Tchapmi, A. Toshev, R. Martín-Martín, and S. Savarese, "Interactive gibson benchmark: A

- benchmark for interactive navigation in cluttered environments,” *IEEE Robotics and Automation Letters*, vol. 5, no. 2, pp. 713–720, 2020.
- [12] Manolis Savva*, Abhishek Kadian*, Oleksandr Maksymets*, Y. Zhao, E. Wijmans, B. Jain, J. Straub, J. Liu, V. Koltun, J. Malik, D. Parikh, and D. Batra, “Habitat: A Platform for Embodied AI Research,” in *Proceedings of the IEEE/CVF International Conference on Computer Vision (ICCV)*, 2019.
- [13] E. Kolve, R. Mottaghi, W. Han, E. Vanderbilt, L. Weihs, A. Herrasti, D. Gordon, Y. Zhu, A. Gupta, and A. Farhadi, “Ai2-thor: An interactive 3d environment for visual ai,” *arXiv preprint arXiv:1712.05474*, 2017.
- [14] E. Wijmans, S. Datta, O. Maksymets, A. Das, G. Gkioxari, S. Lee, I. Essa, D. Parikh, and D. Batra, “Embodied Question Answering in Photorealistic Environments with Point Cloud Perception,” in *Proceedings of the IEEE Conference on Computer Vision and Pattern Recognition (CVPR)*, 2019.
- [15] P. Ammirato, P. Poirson, E. Park, J. Kosecka, and A. C. Berg, “A dataset for developing and benchmarking active vision,” in *IEEE International Conference on Robotics and Automation (ICRA)*, 2017.
- [16] S. Shah, D. Dey, C. Lovett, and A. Kapoor, “Airsim: High-fidelity visual and physical simulation for autonomous vehicles,” in *Field and Service Robotics*, 2017. [Online]. Available: <https://arxiv.org/abs/1705.05065>
- [17] A. Dosovitskiy, G. Ros, F. Codevilla, A. Lopez, and V. Koltun, “CARLA: An open urban driving simulator,” in *Proceedings of the 1st Annual Conference on Robot Learning*, 2017, pp. 1–16.
- [18] NVIDIA Corporation, “Nvidia isaac: The platform for robotics,” 2019, accessed: 31-07-20. [Online]. Available: <https://www.nvidia.com/en-au/deep-learning-ai/industries/robotics/>
- [19] J. Sturm, N. Engelhard, F. Endres, W. Burgard, and D. Cremers, “A benchmark for the evaluation of rgb-d slam systems,” in *2012 IEEE/RSJ International Conference on Intelligent Robots and Systems*. IEEE, 2012, pp. 573–580.
- [20] R. Mur-Artal and J. D. Tardós, “Orb-slam2: An open-source slam system for monocular, stereo, and rgb-d cameras,” *IEEE Transactions on Robotics*, vol. 33, no. 5, pp. 1255–1262, 2017.
- [21] T. Whelan, R. F. Salas-Moreno, B. Glocker, A. J. Davison, and S. Leutenegger, “Elasticfusion: Real-time dense slam and light source estimation,” *The International Journal of Robotics Research*, vol. 35, no. 14, pp. 1697–1716, 2016.
- [22] J. Czarnowski, T. Laidlow, R. Clark, and A. J. Davison, “Deepfactors: Real-time probabilistic dense monocular slam,” *IEEE Robotics and Automation Letters*, vol. 5, no. 2, pp. 721–728, 2020.
- [23] M. Runz, M. Buffier, and L. Agapito, “Maskfusion: Real-time recognition, tracking and reconstruction of multiple moving objects,” in *2018 IEEE International Symposium on Mixed and Augmented Reality (ISMAR)*. IEEE, 2018, pp. 10–20.
- [24] D.-C. Hoang, T. Stoyanov, and A. J. Lilienthal, “High-quality instance-aware semantic 3d map using rgb-d camera,” *arXiv preprint arXiv:1903.10782*, 2019.
- [25] M. Grinvald, F. Furrer, T. Novkovic, J. J. Chung, C. Cadena, R. Siegwart, and J. Nieto, “Volumetric instance-aware semantic mapping and 3d object discovery,” *IEEE Robotics and Automation Letters*, vol. 4, no. 3, pp. 3037–3044, 2019.
- [26] G. Narita, T. Seno, T. Ishikawa, and Y. Kaji, “Panopticfusion: Online volumetric semantic mapping at the level of stuff and things,” *arXiv preprint arXiv:1903.01177*, 2019.
- [27] R. Hachiuma, C. Pirchheim, D. Schmalstieg, and H. Saito, “Detectfusion: Detecting and

- segmenting both known and unknown dynamic objects in real-time slam,” *arXiv preprint arXiv:1907.09127*, 2019.
- [28] R. Kümmerle, G. Grisetti, H. Strasdat, K. Konolige, and W. Burgard, “o: A general framework for graph optimization,” in *Proceedings of the 2011 IEEE International Conference on Robotics and Automation*, 2, pp. 3607–3613.
- [29] M. Kaess, H. Johannsson, R. Roberts, V. Ila, J. Leonard, and F. Dellaert, “isam2: Incremental smoothing and mapping with fluid re-linearization and incremental variable reordering,” in *2011 IEEE International Conference on Robotics and Automation*. IEEE, 2011, pp. 3281–3288.
- [30] P. Krauthausen, A. Kipp, and F. Dellaert, “Exploiting locality in slam by nested dissection.” Georgia Institute of Technology, 2006.
- [31] A. Geiger, P. Lenz, and R. Urtasun, “Are we ready for autonomous driving? the kitti vision benchmark suite,” in *2012 IEEE Conference on Computer Vision and Pattern Recognition*. IEEE, 2012, pp. 3354–3361.
- [32] L. Nicholson, M. Milford, and N. Sünderhauf, “Quadricslam: Dual quadrics from object detections as landmarks in object-oriented slam,” *IEEE Robotics and Automation Letters*, vol. 4, no. 1, pp. 1–8, 2018.
- [33] Z. Liao, W. Wang, X. Qi, X. Zhang, L. Xue, J. Jiao, and R. Wei, “Object-oriented slam using quadrics and symmetry properties for indoor environments,” *arXiv preprint arXiv:2004.05303*, 2020.
- [34] A. Mousavian, D. Anguelov, J. Flynn, and J. Kosecka, “3d bounding box estimation using deep learning and geometry,” in *Proceedings of the IEEE Conference on Computer Vision and Pattern Recognition*, 2017, pp. 7074–7082.
- [35] S. Yang and S. Scherer, “Cubeslam: Monocular 3-d object slam,” *IEEE Transactions on Robotics*, vol. 35, no. 4, pp. 925–938, 2019.
- [36] J. Hou, A. Dai, and M. Nießner, “3d-sis: 3d semantic instance segmentation of rgb-d scans,” in *Proceedings of the IEEE Conference on Computer Vision and Pattern Recognition*, 2019, pp. 4421–4430.
- [37] C. R. Qi, O. Litany, K. He, and L. J. Guibas, “Deep hough voting for 3d object detection in point clouds,” in *Proceedings of the IEEE International Conference on Computer Vision*, 2019, pp. 9277–9286.
- [38] Z. Yang, Y. Sun, S. Liu, and J. Jia, “3dssd: Point-based 3d single stage object detector,” in *Proceedings of the IEEE/CVF Conference on Computer Vision and Pattern Recognition*, 2020, pp. 11 040–11 048.
- [39] D. Hall, F. Dayoub, J. Skinner, H. Zhang, D. Miller, P. Corke, G. Carneiro, A. Angelova, and N. Sünderhauf, “Probabilistic object detection: Definition and evaluation,” in *The IEEE Winter Conference on Applications of Computer Vision*, 2020, pp. 1031–1040.
- [40] B. Talbot, D. Hall, H. Zhang, S. R. Bista, R. Smith, F. Dayoub, and N. Sünderhauf, “Benchbot: Evaluating robotics research in photorealistic 3d simulation and on real robots,” *arXiv preprint arXiv:2008.00635*, 2020.